Changes in Ice-Flow Velocity and Surface Elevation from 1874 to 2006 in Rhonegletscher, Switzerland

Daisuke Nishimura*†§

Shin Sugiyama*

Andreas Bauder‡ and

Martin Funk‡

*Institute of Low Temperature Science, Hokkaido University, Nishi-8 Kita-19 Sapporo, Japan
†Graduate School of Environmental Science, Hokkaido University, Nishi-5 kita-10, Japan
‡Section of Glaciology, Versuchsanstalt für Wasserbau, Hydrologie und Glaziologie (VAW), ETH Zürich, Gloriastrasse 37/39, 8092 Zürich, Switzerland
§Corresponding author: ndaisuke@lowtem.hokudai.ac.jp

Abstract

We have studied changes in the ice-flow velocity and ice thickness in Rhonegletscher, Switzerland, over the period 1874–2006. The flow velocity field and surface elevation were analyzed in the lower half of the glacier using aerial photograph pairs taken in 1970/1971, 1981/1982, 1999/2000, and 2005/2006. We also digitized velocities measured by Mercanton (1916) in 1874–1910 by tracking stones distributed on the glacier. The results showed that the ice-flow velocity and ice straining conditions were strongly influenced by changes in the glacier geometry over the last 100 years. For example, the longitudinal strain rate near the current terminus has changed from tensile to compressive since the retreat of the glacier over a steep bedrock slope to a relatively flat region. The velocity decreased over the studied region from 1981 to 2006, which is in agreement with the ice thinning during the same period. However, the rate of the velocity change was smaller in the post-1990 period, because the effect of the thinning on ice flow speed was partly canceled out by the effect of steepening of the ice surface. The velocity change also implied that the magnitude of basal ice motion was influenced by changing subglacial drainage conditions and proglacial lake formation. Our unique data set contributes to a better understanding of ice dynamics under changing glacier geometry.

Introduction

Mass loss from mountain glaciers is contributing to the rise in global sea levels (e.g., Meier et al., 2007). Thus, an accurate assessment of the evolution of glaciers in the past and future is urgently needed. The mass changes of a glacier are given by the balance of accumulation and ablation, but the dynamic response to the changing climate cannot be predicted without an understanding of the ice dynamics. Snow and ice accumulate upglacier and move down to the lower reaches, where ice dissipates by melting and calving. Spatial distributions of ice velocity cause straining of ice, which controls glacier surface evolution together with the surface mass balance. Subsequent changes in ice thickness and surface slope then affect the ice dynamics, and changes in surface elevation modify mass balance regimes. Ice dynamics is more directly related to glacier mass budget in the case of calving glaciers as it controls the rate of ice discharge from the calving front. Because of these interactions between ice motion and other glaciological processes, ice flow speed and its spatial and temporal variations play a critical role in the net effect of the mass exchange on the glacier evolution. One example of clear influence of ice dynamics on glacier evolution is recent thinning near the terminus of Glacier d'Argentiere in the French Alps. Vincent et al. (2009) and Berthier and Vincent (2012) compiled field and remote-sensing observations for this glacier dating back to the 1970s and showed that the changing flow regime was the driver for the change in ice thickness at the glacier tongue, rather than the surface mass balance.

After the recognition of glacier flow in the 19th century (summarized in Clarke, 1987), ice-flow velocities were measured in many glaciers worldwide. Intensive velocity measurements in the earlier period include those in Athabasca Glacier in Canada (Paterson and Savage, 1963), Franz Josef Glacier in New Zealand (McSa-veney and Gage, 1968), and Unteraargletscher in Switzerland (Flotron, 1924–2010). The velocity is measured commonly by surveying the displacement of markers fixed on a glacier, typically by using different types of survey instruments (e.g. theodolite, distance meter, and GPS; Hubbard and Glasser, 2005) to measure positions of stakes drilled into snow and ice. The conventional stake method is relatively accurate and convenient for high-frequency measurements but difficult to cover a large area over a glacier with a high spatial resolution. The spatial coverage and resolution can be improved by employing the feature tracking method, in which a sequential image pair is analyzed to measure the displacement of glacier surface features. For instance, the velocity field in the lower part of Columbia Glacier in Alaska has been comprehensively measured for the last several decades (e.g. Krimmel, 2001). The methodology has been automated (e.g. Scambos et al., 1992) and widely applied for aerial photographs and satellite images (e.g. Dowdeswell and Benham, 2003; Kääb, 2005; Quincey et al., 2011).

The glacier flow velocity data are valuable particularly because they serve as important input data for numerical glacier models. Numerical glacier modeling is a powerful tool for reconstructing past glacier geometries and predicting future evolution (e.g. Oerlemans, 1986; Schneeberger et al., 2001; Le Meur et al., 2007; Huss et al., 2007; Yamaguchi et al., 2008). Such models account for the ice dynamics by coupling an ice-flow model with a mass-balance model. Ice flow can be computed with different degrees of complexity, but in any case, observational data are important to determine the parameters needed for the velocity computations. The recent development of sophisticated three-dimensional ice-flow models has enabled the computation of detailed flow velocity fields over glaciers (e.g. Jouvet et al., 2009). The calibration and validation of such models require velocity measurements covering a large area with a high spatial resolution. The feature tracking

method applied for aerial and satellite images is a useful tool to obtain the data set needed for such modeling work. It is also crucial for the accuracy of the model to calibrate its parameters with long-term velocity data, because a parameter set calibrated with data from a single period does not necessarily represent glacier conditions for a longer period. For example, Iken and Truffer (1997) studied ice velocity of Findelengletscher in 1982, 1985, and 1994, and found significantly different relationships between ice speed and subglacial water pressure in each year. This implies that parameters in a sliding law, or the type of sliding law, have changed over the course of the glacier geometry change.

Aerial and satellite images are useful not only for ice velocity measurements, but also for estimating glacier volume changes by measuring surface elevation. Generation of digital elevation models (DEMs) from a stereographic image pair is a well-established technique of photogrammetry (e.g. Kääb and Funk, 1999; Bauder et al., 2007; Barrand et al., 2009), and a comparison of multitemporal DEMs provides spatial distributions of changes in glacier surface elevation. This method is particularly efficient to measure details of ice mass change over a large area, as demonstrated by recent work on Alaskan glaciers (Berthier et al., 2010) and the Patagonia Ice Field (Willis et al., 2012). In addition to DEMs derived by photogrammetry, elevation data from various different sources, e.g. SRTM (Shuttle Radar Topography Mission), ICESat (Ice, Cloud, and land Elevation Satellite), airborne lidar measurements, and old contour maps, are utilized to expand spatial and temporal coverage of ice volume change measurements (e.g. Nuth et al., 2010).

In this study, we present surface velocity and elevation changes in the lower half of Rhonegletscher in the Swiss Alps from 1874 to 2006. This unique data set was obtained by analyzing aerial photographs taken in the period from 1970 to 2006, and compiling the velocity map reported for the period 1874–1915 (Mercanton, 1916). A part of the velocity data set has already been utilized in previous studies for calibrating numerical models of Rhonegletscher (Sugiyama et al., 2007; Jouvet et al., 2009; Goehring et al., 2012). Elevation change of Rhonegletscher during the same period has been studied before to quantify the ice volume change (Bauder et al., 2007). Here we analyze more details of DEMs derived from the materials used in Bauder et al. (2007) and compare elevation changes with ice velocity variations over the same period. Our data illustrate changes in the velocity field over more than 100 years under the influence of rapid retreat and thinning of this valley glacier.

Study Site

Rhonegletscher is a temperate valley glacier in the Swiss Alps (46°37′N, 8°24′E). In 2000, the glacier was 9 km long and covered an area of 16.45 km^2 (Bauder et al., 2007). In the 19th century, the glacier terminus was about 1700 m downglacier from the 2006 terminus position (Sugiyama et al., 2007), forming a piedmont-type glacier tongue at the foot of a steep bedrock slope (Figs. 1 and 2, part a; see Fig. 1, part b, for the location of the steep slope). It has been retreating since the late 19th century, except for a couple
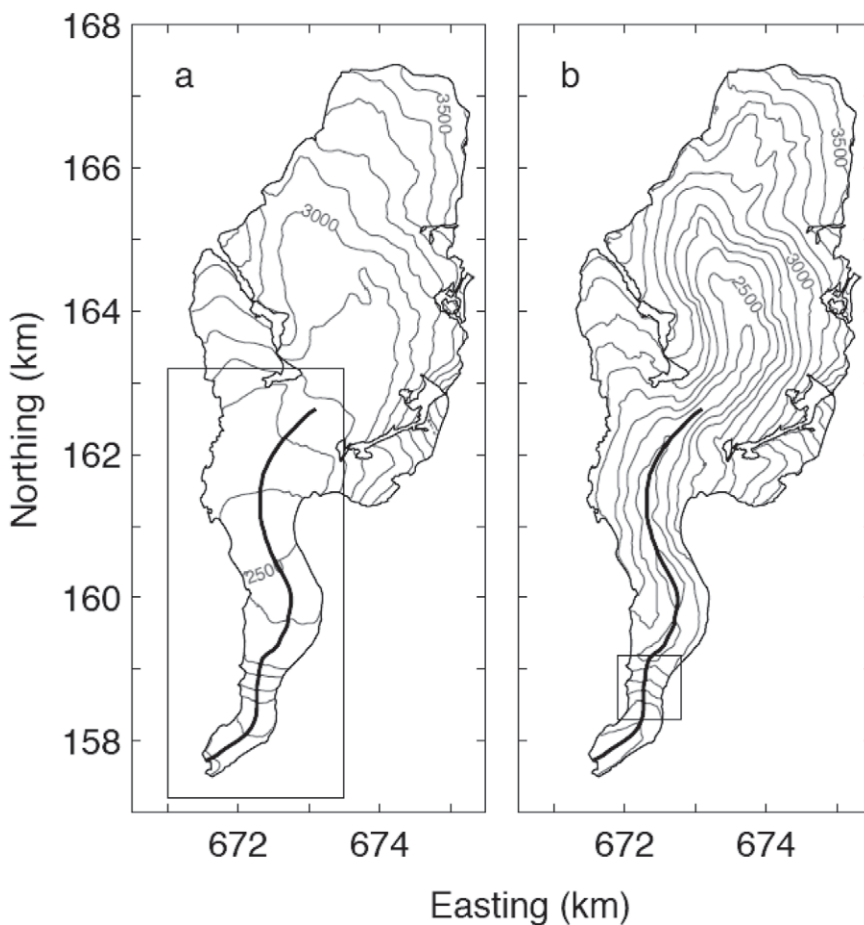

FIGURE 1. Maps of Rhonegletscher showing (a) the surface elevation observed in 1874 and (b) the glacier bed elevation. The contour intervals are 100 m, and the coordinates correspond to the Swiss official coordinate system. The solid line along the valley center is used for the analysis. The boxes in (a) and (b) show the area studied in this paper and the location of a steep bedrock cliff, respectively.

FIGURE 2. Aerial view of Rhonegletscher from the south in (a) 1860 and (b) 1962. The photograph (b) was taken by J. Geiger, and the drawing (a) was constructed on the same photograph by B. Nedera using the results of numerical modeling (Sugiyama et al., 2007).

of short periods of ice front advance (Zahno, 2004; Carlen, 2005; Jouvet et al., 2009; Glaciological Reports, 1881–2011). The current snout is located at the top of the steep slope (Fig. 2, part b). Because the terminus retreated over a bedrock bump, a proglacial lake has formed since 2005 at the depression between the bump and the glacier (Sugiyama et al., 2008; Tsutaki et al., 2011, 2013). In this study, we focus our analysis on the lower 6 km from the 1874 terminus position (Fig. 1, part a), for which ice velocity data from the 19th century are available and ice surface features allow us to process aerial photographs by a photogrammetric method.

Rhonegletscher has one of the longest histories of glaciological investigations in the world. The annual mass balance was measured by stake measurements for the periods 1874–1875, 1885–1910 (Mercanton, 1916), and 1980–1982 (Chen and Funk, 1990). Ice volume changes during the period 1874–2000 were studied by comparing six DEMs generated from maps and aerial photographs (Bauder et al., 2007). These data of the changes in ice volume were utilized to calculate the mass balance history of this glacier using a distributed temperature-index melt model (Huss et al., 2008). A bedrock elevation map was constructed from an ice-radar survey carried out in 2003 (Zahno, 2004) and boreholes drilled in 2007–2009 (Sugiyama et al., 2008; Tsutaki et al., 2011)

(Fig. 1, part b). One-dimensional flowline models have been applied to this glacier to simulate historical front variations (Stroeven et al., 1989; Wallinga and van de Wal, 1998; Sugiyama et al., 2007; Goehring et al., 2012). For example, Sugiyama et al. (2007) have studied the evolution of Rhonegletscher over the last 125 years and into the future using a model improved by accounting for ice-flow fields across the glacier. More recently, the retreat history of Rhonegletscher was utilized to investigate the drivers of glacier evolution in the Alps (Goehring et al., 2012). A three-dimensional glacier model was also applied to Rhonegletscher, and its evolution since 1874 was successfully reproduced by the model simulation (Jouvet et al., 2009). The authors of these three modeling works tuned their ice-flow models using a part of the velocity data presented in this study.

Method

AERIAL PHOTOGRAPH ANALYSIS

Surface elevation and horizontal ice velocities were measured by analyzing aerial photographs. The photographs of the lower half of Rhonegletscher were taken by the Swiss Federal Office of Topography from 1970 to 2006. The upper half of the glacier was excluded from the analysis since the snow-covered surface provides no distinct features required for the methods described below. Black-and-white positive films were used for the aerial photography. The image scales, which are dependent on the flight height, lens system, and type of the film, were 1:16,000 for the photographs taken from 1970 to 1982 and 1:10,000 for those taken from 1999 to 2006. The specific dates and other information of the photographs are summarized in Table 1.

We employed a stereophotogrammetric method (e.g. Kääb and Funk, 1999; Barrand et al., 2009) to generate DEMs and velocity fields from the aerial photographs. DEMs were generated for 1970, 1971, 1981, 1982, 1999, 2000, 2005, and 2006 by processing pairs of overlapping photographs taken from different airplane positions. The analysis was carried out with a computer-aided photogrammetric compilation system, an analytical stereo plotter (DSR15–18, KERN), and the corresponding computer software for this device (apx 6.3, AVIO SOFT). The positive films were mounted on the

TABLE 1

Aerial photographs used in this study.

Year	Date	Analyzed for	Number of GCPs	Scale
1970	18 September	Elevation change/ Velocity	4	1:16,000
1971	17 August	Velocity	4	1:16,000
1981	18 September	Elevation change/ Velocity	4	1:16,000
1982	13 September	Velocity	4	1:16,000
1999	9 September	Elevation change/ Velocity	16	1:10,000
2000	23 August	Velocity	16	1:10,000
2005	15 September	Velocity	16	1:10,000
2006	5 September	Elevation change/ Velocity	16	1:10,000

analytical stereo plotter and processed to measure surface elevation at grid points of a 100-m-resolution mesh. More details of the method are described in Kääb et al. (1997) and Kääb and Funk (1999). Geometrical corrections were performed as below. After correcting film distortions using markers on film corners (fiducial marks), we generated a photomosaic composed of 5–15 photographs to cover the entire study area for each year. To overlap the photographs accurately, we superimposed 12–20 characteristic surface features identified on neighboring images. The mosaics were geometrically corrected using GCPs (ground control points), which were painted on the bedrock around the glacier. Four GCPs were available for the years between 1970 and 1982, and 16 between 1999 and 2006. For these correction processes, we utilized digital photogrammetry software, the Leica Photogrammetry Suite, and ORIMA, implemented in ERDAS IMAGINE 8.7 (Leica Geosystems). Based on the flight height of the aerial photography in the order of 1000–3000 m above the surface, the accuracy of the DEMs was expected to be ± 0.3 m. This estimation was validated by Bauder et al. (2007) in the study performed using the same GCPs, by comparing DEMs over the terrain outside of the glacier. We considered only the flat glacier surface (slopes below 20%) for our analysis to avoid artifacts from horizontal shifts. The DEMs we obtained were compared at the grid points of 100-m-resolution mesh, and elevation changes were averaged over the glacier surface covered by the DEMs. We also evaluated elevation changes along the glacier centerline (see Fig. 1) by linear interpolation of the DEMs.

The photographs were superimposed on those taken in subsequent years to measure the displacement of characteristic surface features such as crevasses and boulders. This measurement was performed on the same system as the stereophotogrammetric DEM analysis. We measured the displacement by overlapping a photograph view on the other one taken in the next year by operating the stereo plotter (Kääb et al., 1997; Kääb and Funk, 1999).The measurements were made at every grid point of a 100-m mesh unless no traceable feature was available. The accuracy of the velocity measurements is highly dependent on the image quality of the target. Thus, we repeated the measurements twice for the 1970–1971 pair and compare the velocities at each grid point. The root mean square error between the two measurements was 4.2 m a^{-1}. The accuracy of the velocities obtained in this study was also evaluated by comparing our data with field measurements, which were carried out in 2006 and 2007 by surveying 7 stakes installed along the glacier centerline with a theodolite (Turi, 2009). Accuracy of this field velocity measurement was better than 1 m a^{-1}. The mean deviation of our data from the field data was 4 m a^{-1}.

REANALYSIS OF MERCANTON'S DATA

During the period 1874–1915, Mercanton (1916) measured ice motion by tracking stones and slats distributed over the glacier surface. The markers were placed every 20 m along four profiles across the lower half of the glacier. Mercanton and his colleagues surveyed these markers every year in late August or early September by triangulation, and marker locations were indicated on a 1:5000 map. We scanned the velocity map and digitized the coordinates of the stones using digitization software. The accuracy of Mercanton's measurements is not clear, but the accuracy of triangu-

lation by theodolite measurements is usually within several centimeters. The stones used for the measurement were head sized, thus we expect about 0.3 m of uncertainty in the surveyed positions. The markers could have slid from the original position, which might have introduced an additional uncertainty of 1 m. Errors introduced in the scanning and digitization procedures were less than 3 m. Therefore, we estimate an accuracy better than 5 m a^{-1} for the velocities measured by Mercanton and compiled in this study. This accuracy is similar with that estimated for the measurement with aerial photographs in this study. A 25-m resolution DEM was generated by Zahno (2004) from a map constructed in 1874 (Mercanton, 1916) and was used to analyze glacier surface elevation in this study.

Results and Discussion

SURFACE ELEVATION

We compared the DEMs for 1874, 1970, 1981, 1999, and 2006 to compute the elevation changes over the periods. Surface elevations for 1874 and 2006, and elevation change over the 132 years are shown in Figure 3. The glacier ice completely disappeared in the lower reaches of the steep slope, and the glacier width decreased in the studied region (Fig. 3, parts a and b). Besides the complete loss of more than 100-m-thick ice at the foot of the slope, about 100 m of thinning was observed near the 2006 terminus (Fig. 3, part c). The marked ice thinning observed at two locations in the upper reaches near the margins was due to the recession of tributary glaciers. The magnitude of the thinning generally increases downglacier along the centerline (Fig. 4 and Table 2). For example, the change in thickness from 1874 to 2006 was -75 m in the region near the 2006 terminus ($x = 1800$–3300 m, where x is the distance from the 1874 terminus), whereas it was -45 m in the uppermost region of the analyzed area ($x = 4800$–6300 m). The thinning rate was not uniform over the study period, as summarized in Table 2. Near the 2006 terminus ($x = 1800$–3300 m), the glacier thinned at a rate of 0.40 m a^{-1} over the period 1874–1970, and then the thinning rate increased to 1.05 m a^{-1} in the period 1970–2006. Thinning rates in the upper reaches ($x = 4800$–6300 m) for the same periods were 0.27 and 0.56 m a^{-1}, respectively. It should be noted that the thinning rate between 1874 and 1970 is a relatively longer term average than the other periods. Nevertheless, these results indicate a significant increase in the thinning rate after 1981, and thinning after 1981 accounts for more than 50% of total thinning since 1874. Before the initiation of the rapid thinning, thickness slightly increased from 1970 to 1981.

Maps of the elevation change rates over the study area show more details of spatial and temporal variability (Fig. 5). The thinning rate was relatively uniform over the study area in 1874–1970 (Fig. 5, part a). Clear spatial variations, i.e. greater thinning rate downglacier, are visible in the maps for 1981–1999 and 1999–2006 (Fig. 5, parts c and d). The mean rate of thinning over the area was 0.34 m a^{-1} in 1874–1970. It increased after 1981 and reached 1.73 m a^{-1} in 1999–2006 (Table 2). The thinning due to the retreat of the tributary was most significant in 1981–1999 (Fig. 5, part c). The slight elevation increase from 1970 to 1981 was pronounced at the middle part of the studied region (Fig. 5, part b).

These spatial and temporal variations in the rate of ice thickness change are consistent with previous studies. Bauder et al.
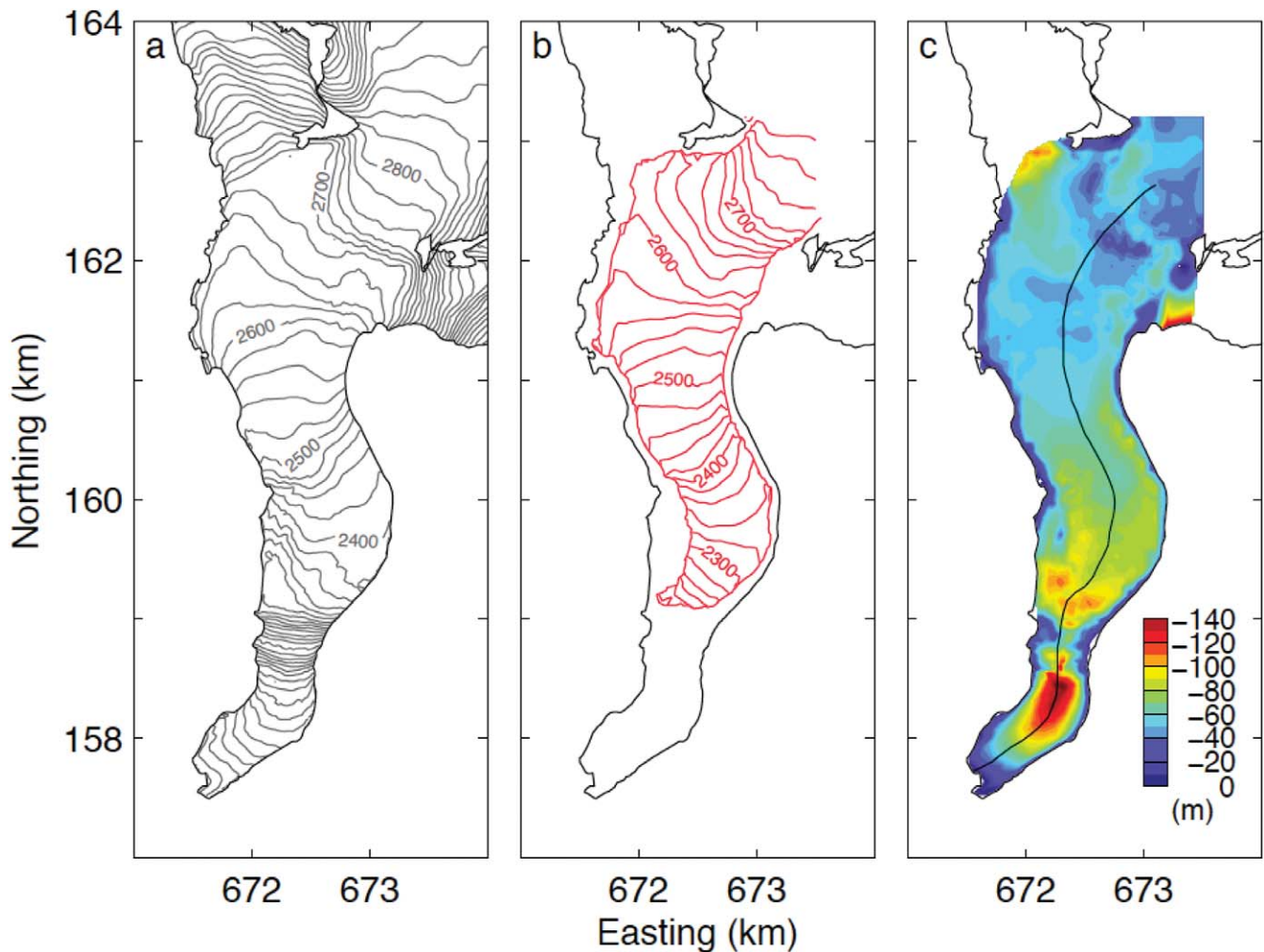
FIGURE 3. Surface elevation in (a) 1874 and (b) 2006 (contour intervals 20 m), and glacier margins in (a) 1874 and (b) 2008. (c) Surface elevation change from 1874 to 2006. The solid line in (c) is the central flowline used for the analysis. The coordinates correspond to the Swiss official coordinate system.

(2007) studied surface elevation changes of 19 glaciers in the Swiss Alps, including Rhonegletscher. They reported that the thickness change was small in the accumulation area and largest near the glacier snout, as we observed in this study. Huss et al. (2008) reported a slightly positive mass change from 1960 to 1980 followed by an increasing rate of mass loss from 1980 to 2000. Tsutaki et al. (2013) found that ice thinning rate increased near the terminus after 2006 under the influence of proglacial lake formation. This indicates that ice thinning accelerated even after the doubling of the thinning rate from 1981–1999 to 1999–2006.

ICE-FLOW VELOCITIES

Figure 6 shows surface flow velocity fields obtained for the periods 1970/1971, 1981/1982, 1999/2000, and 2005/2006. The velocity generally increased from 1970/1971 to 1981/1982, and then decreased from 1981/1982 to 1999/2000 as the glacier retreated. The maximum velocities over the four periods are 124, 125, 103, and 101 m a^{-1}, respectively. The location of this maximum is up-glacier at the valley center where the ice is thick, and there is no substantial change in the location over the period (Fig. 6). The

surface flow velocity decreases downglacier and towards the glacier margins as the ice thickness decreases. The direction of the ice flow is approximately parallel to the valley wall.

The velocity map for 1874–1915 displays the ice-flow field in the currently ice-free region (south of 159 km in Swiss coordinate northing) as well as the lower half of the area analyzed using the aerial photographs (Fig. 7). The greatest velocity in this period was observed at the steep slope, several hundred meters downglacier from the 2006 terminus. The velocities were 127, 204, and 76 m a^{-1} at the head, middle, and foot of the slope, respectively (indicated in Fig. 6 as A, B, and C). The velocity decreased below the cliff towards the terminus. It was less than 13 m a^{-1} at the lowermost profile, about 400 m from the terminus.

Velocity profiles along the glacier centerline (see Fig. 1) are compared in Figure 8. From the 19th to the 20th century a notable change occurred in the longitudinal velocity pattern near the 2006 terminus. Within the region $x = 2000$–4000 m from the 1874 terminus, the flow velocity was greater downglacier during the period between 1874 and 1915, indicating a strongly extending flow regime. After the ice retreated beyond the steep slope in the 20th century, the longitudinal flow regime was compressive, i.e.,
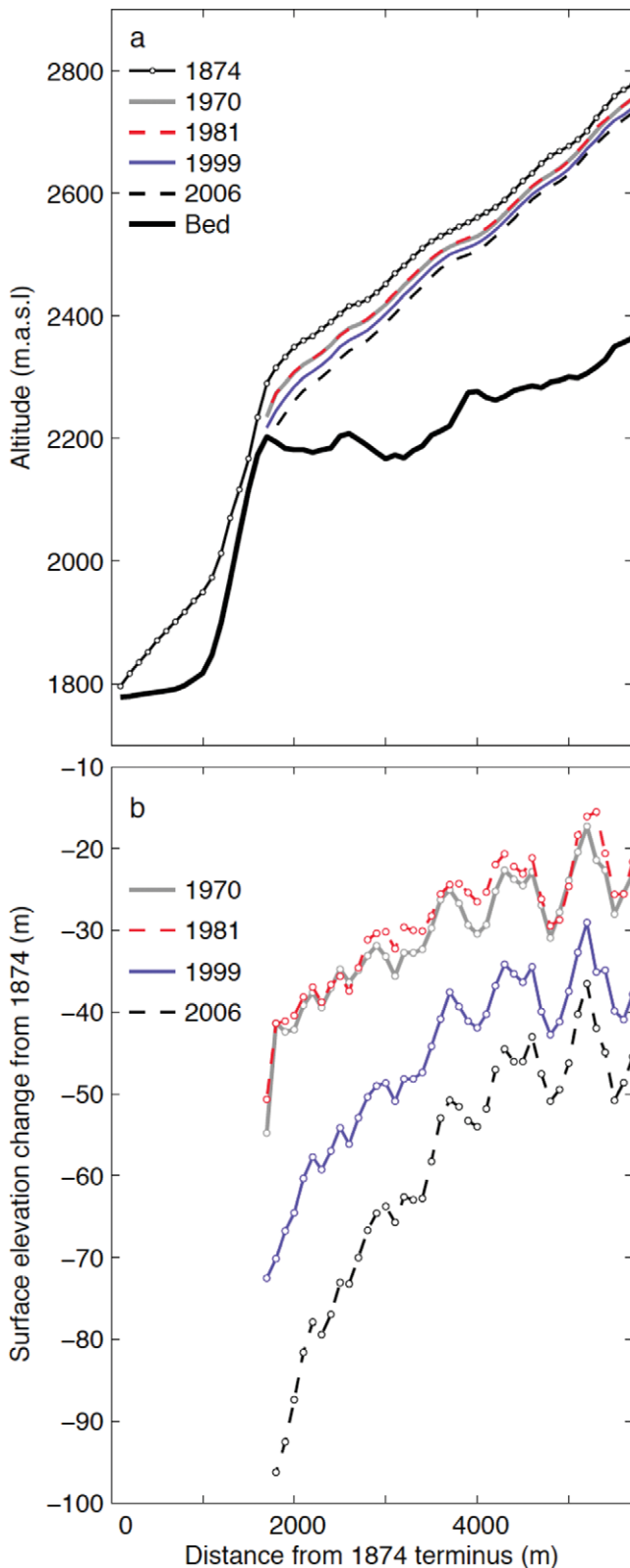
FIGURE 4. (a) Ice surface elevations in 1874, 1970, 1981, 1999, and 2006 along the glacier centerline indicated in Figures 1 and 3, part c. The thick black curve shows the bedrock elevation. **(b)** The change in surface elevation along the glacier centerline from 1874 to 1970, 1981, 1999, and 2006.

TABLE 2

Mean thinning rates obtained for the study periods. Spatial means were computed for the lower and upper reaches along the central flowline, and over the entire areas shown in Figure 5. The lower and upper reaches are defined as $x = 1800-3300$ and $4800-6300$ m (x is the distance from the 1878 terminus position), respectively.

	Mean thinning rate (m a^{-1})			
Period	1878–1970	1970–1981	1981–1999	1999–2006
Upper flowline	0.26	−0.12	0.74	1.17
Lower flowline	0.38	−0.11	1.13	2.67
Study area	0.33	−0.15	0.87	1.73

the velocity progressively decreased downglacier. This change in the flow regime would have played a key role in causing changes in the ice thickness by switching the vertical strain rate from negative to positive. Although the overall flow velocity changed between 1970 and 2006, the longitudinal flow regime remained the same. The velocity slightly increased from 1970/1971 to 1981/1982, followed by a relatively rapid speed reduction from 1981/1982 to 1999/2000. It appears that these velocity changes after 1970 correspond to the slight thickening from 1970 to 1981 followed by the rapid thinning until 2006, as described in the previous subsection. The influence of the glacier geometry change on the ice dynamics is investigated more in detail below.

VELOCITY CHANGES UNDER CHANGING GLACIER GEOMETRY

To investigate the effect of changing glacier geometry on the ice dynamics, we analyzed changes in ice thickness, surface slope, and ice velocity during the glacier retreat starting in the 1980s. Glacier flow is primarily controlled by ice deformation due to horizontal shear stresses and basal ice motion. Assuming ice deforms in simple shear, glacier surface velocity is given by

$$u_s = u_b + \frac{2A}{n+1}(pgH \sin \alpha)^n H, \qquad (1)$$

where u_b is the basal velocity, ρ is the ice density, g is the gravitational acceleration, H is the ice thickness, and α is the downglacier surface slope (Cuffey and Paterson, 2010). The rate factor A and exponent n are parameters in Glen's flow law. By taking a commonly assumed value $n = 3$, the second term of Equation (1) is proportional to H^4 and $(\sin\alpha)^3$. This indicates the ice velocity is highly dependent on the ice thickness and surface slope. Thus, the decrease in the velocity from 1981/1982 to 2006/2007 (Fig. 9, part a) can be attributed to glacier thinning during the same period (Fig. 9, part b). However, since ice motion is controlled by the surface slope as well, the velocity change cannot be directly connected to the change in ice thickness. The situation in Rhonegletscher is not straightforward. The mean change in ice thickness along the longitudinal profile was −10% for both the periods from 1981 to 1999 and 1999 to 2006. Thus, one can expect similar impact on the ice velocity in the two periods [34% reduction according to Equation (1)], but the velocity change was much smaller in the latter period (−28% in 1981–1999 and −11% in 1999–2006) (Figs. 8 and 9, part a). This is partly because the effect of ice thinning on the ice flow was compensated by steepening of the ice
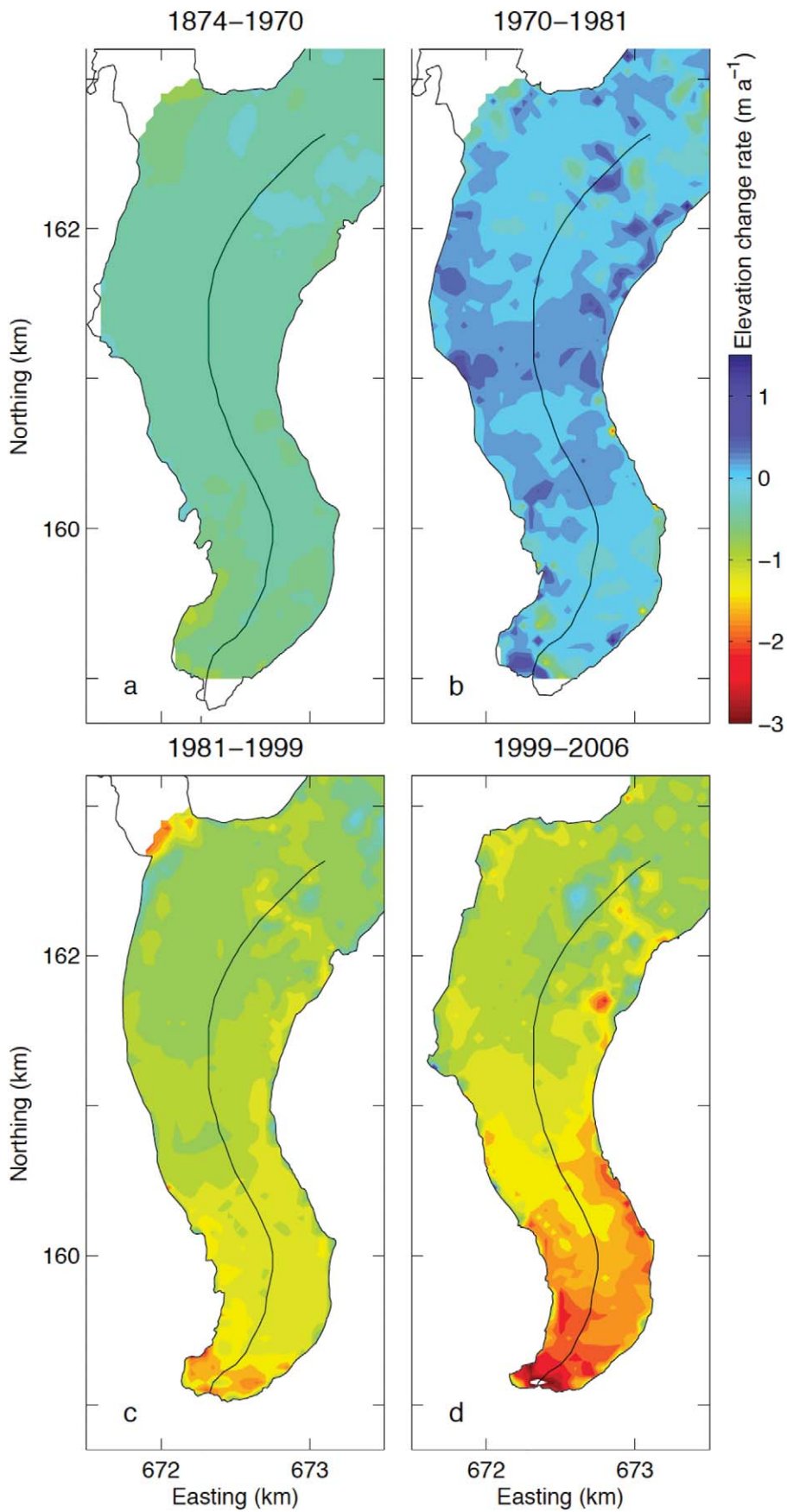
FIGURE 5. The rates of ice surface elevation change for the periods (a) 1874–1970, (b) 1970–1981, (c) 1981–1999, and (d) 1999–2006. The solid lines are the central flowline used for the analysis. The glacier boundaries are drawn based on the aerial photographs taken in (a) 1959, (b) 1980, (c) 2000, and (d) 2008.
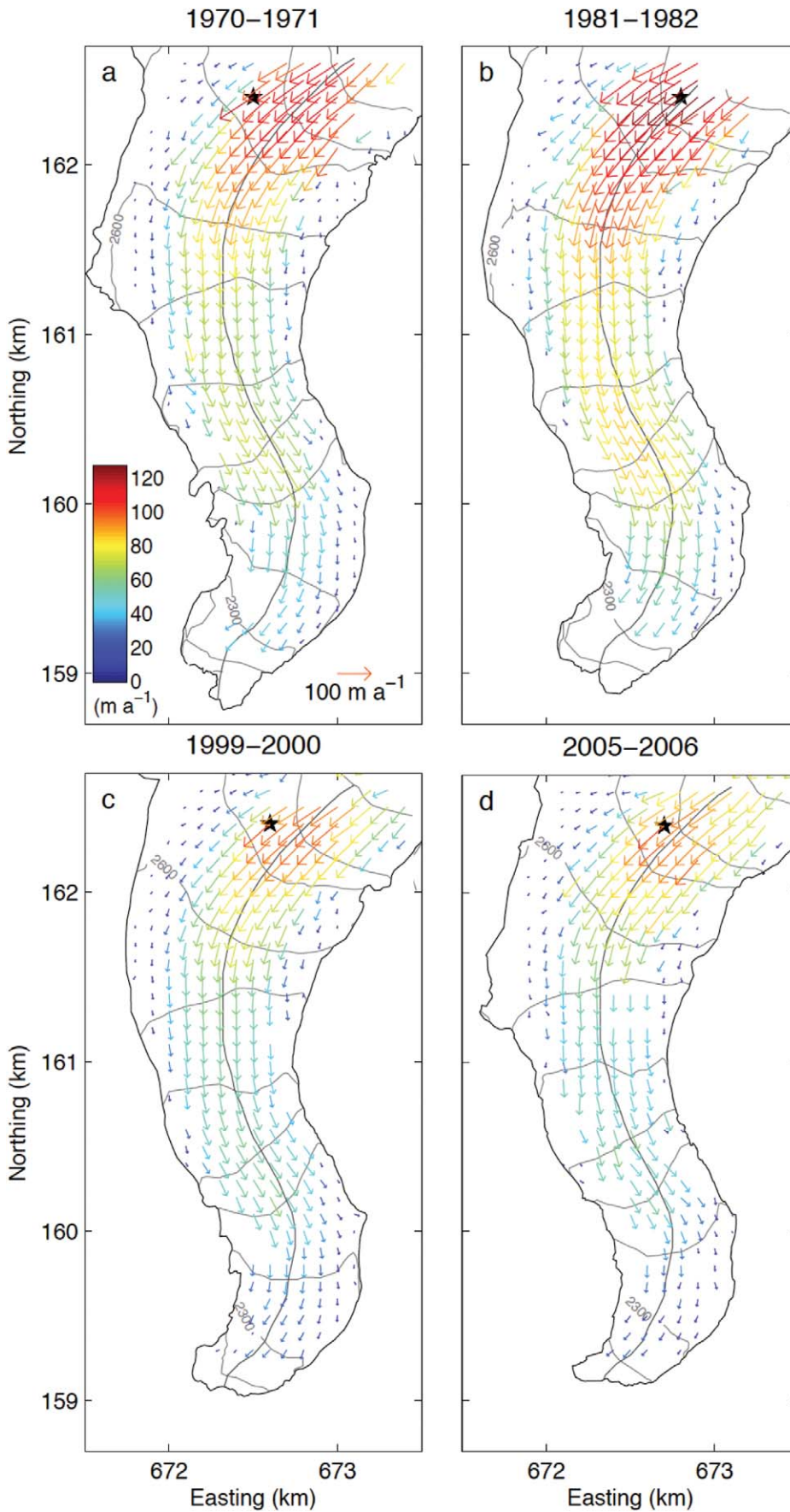
FIGURE 6. Surface flow vectors in (a) 1970/1971, (b) 1981/1982, (c) 1999/2000, and (d) 2005/2006. The contour lines indicate 50-m surface elevation intervals in (a) 1970, (b) 1981, (c) 1999, and (d) 2005. The coordinates correspond to the Swiss official coordinate system. The glacier boundaries are drawn based on the aerial photographs taken in (a) 1959, (b) 1980, (c) 2000, and (d) 2008. The stars indicate the location of the maximum velocities.
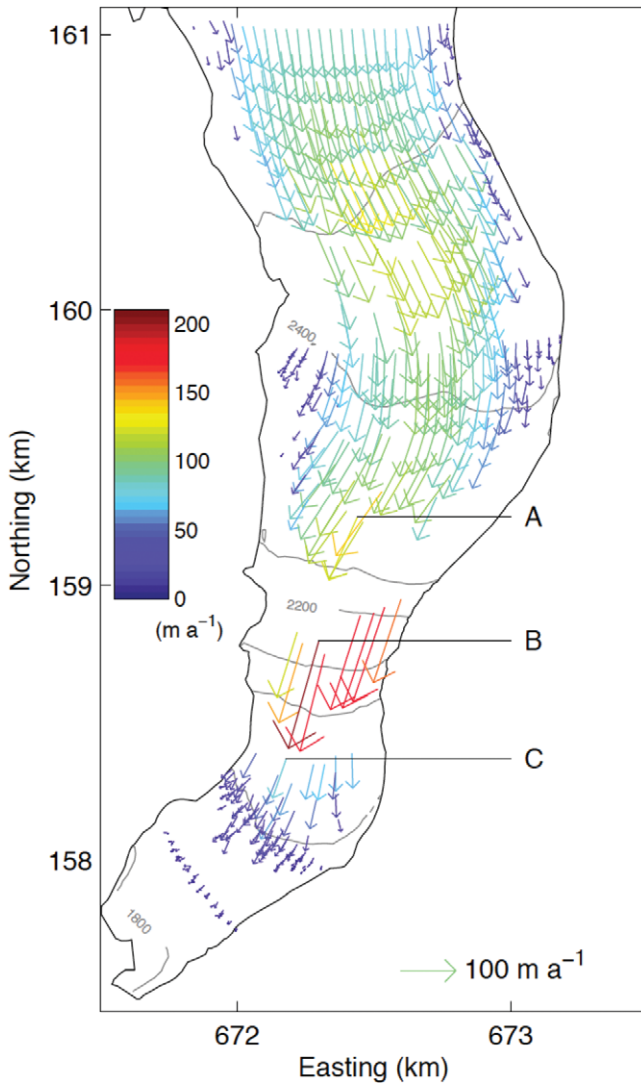
FIGURE 7. Surface flow vectors in 1874/1915 obtained by digitizing Mercanton's map (Mercanton, 1916). The contour lines show 100-m surface elevation intervals observed in 1874. The top, middle, and foot of the steep cliff are indicated by A, B, and C. The coordinates correspond to the Swiss official coordinate system.
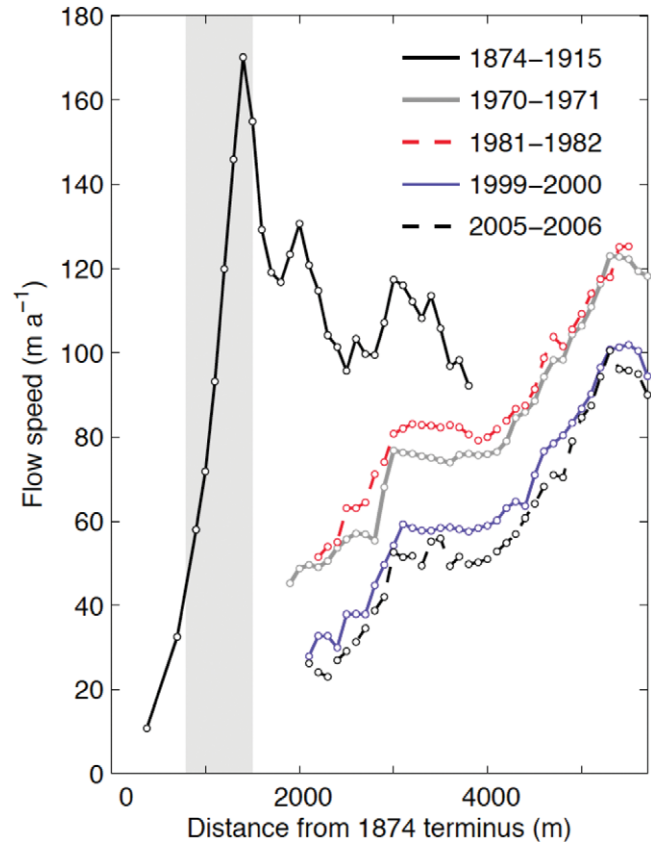

FIGURE 8. Surface flow velocities along the glacier centerline (see Figs. 1 and 3, part c) in 1874/1915, 1970/1971, 1981/1982, 1999/2000, and 2005/2006. The shaded region indicates the steep bedrock slope.

surface slope. The ice thickness decreased from 1981 to 2006, while the surface slope increased over this period, particularly near the terminus (Fig. 9, part b). The change in the slope at $x = 3000–5500$ m was $+0.08°$ from 1981 to 1999 and $+0.14°$ from 1999 to 2006. The steepening trend was more significant in the later period near the terminus ($x = 1900–3000$ m) as well, where the changes were $+0.33°$ and $+0.39°$ for the periods 1981–1999 and 1999–2006, respectively.

Another interpretation of the more substantial slow down from 1981 to 1999 is the change in the subglacial hydraulic conditions over the course of glacier advance and retreat. Iken and Truffer (1997) observed decrease in ice velocity for a given subglacial water pressure in Findelengletscher, Switzerland, between 1982 and 1994. They attributed the deceleration to different types of basal drainage systems before and after the glacier advance peaked in 1981. During the glacier advance, large drainage conduits were destroyed by active ice motion, and numerous smaller channels were formed at the glacier bed. Since such subglacial conditions are favorable for basal sliding, contribution of the sliding to the surface velocity increased. When the glacier began to retreat and ice became less active, the drainage conduits grew larger and the number of individual conduits decreased. Sliding speed is expected to decrease under such subglacial conditions. Rhonegletscher had advanced until 1980, and then began to retreat rapidly in 1988 (Swiss Glacier Monitoring Network, 1881–2011). Presumably, the above-mentioned changes in the drainage condition took place between 1981 and 1999, resulting in the enhanced deceleration during this period. Ice velocity change during a retreat/advance cycle was observed, and its mechanisms have been discussed in some other glaciers (Span and Kuhn, 2003; Herman et al., 2011).

It is also likely that the velocity observed in 2005/2006 was already influenced by the formation of a proglacial lake. It has been reported that the flow speed has increased near the glacier terminus since the formation of the lake in 2005 (Tsutaki et al., 2011, 2013). Thus, velocity decrease from 1999 to 2006 was partially compensated by the basal ice motion enhanced by the lake formation. Only a few observations have been reported on the effects of proglacial lake formation on ice dynamics and terminus retreat (Kirkbride and Warren, 1999; Canassy et al., 2011). Evolution of Rhonegletscher will be more influenced by the lake for the next decades, and thus observations in the future will provide an insight into complex interactions between ice flow and thickness changes under the influence of lake expansion.
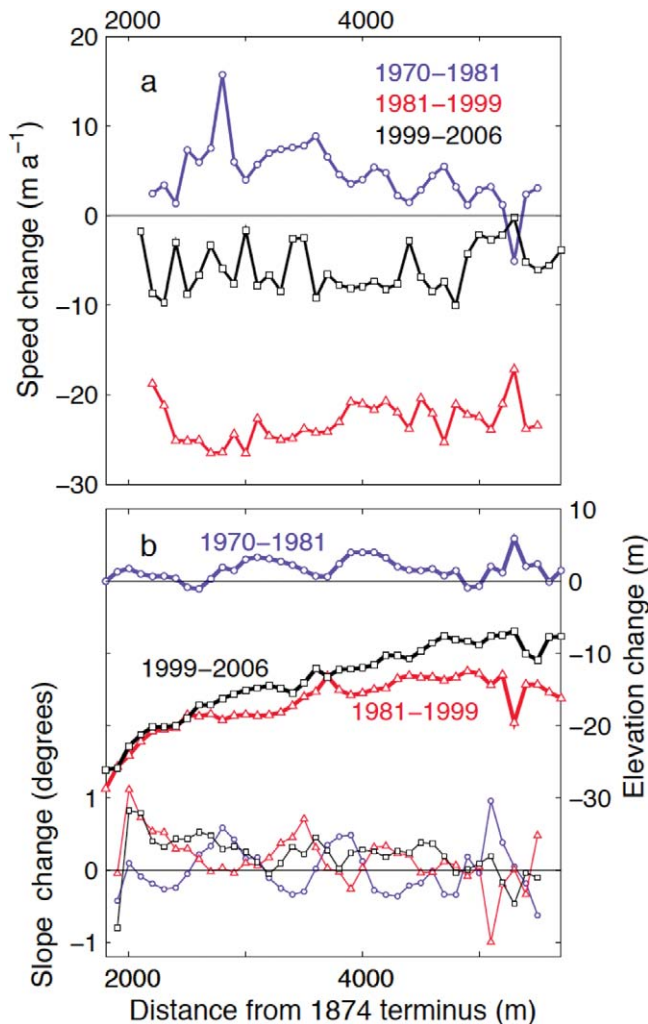
FIGURE 9. (a) Change in surface flow speed along the glacier centerline from 1970 to 1981 (○), 1981 to 1999 (△), and 1999 to 2006 (□). (b) Changes in surface elevation (bold) and ice surface slope (thin) along the glacier centerline from 1970 to 1981 (○), 1981 to 1999 (△), and 1999 to 2006 (□).

Our data collected on Rhonegletscher suggest that the long-term changes in the ice velocity are as a result of various processes. Ice dynamics are controlled not only by glacier geometry, but also by changes in subglacial hydraulic conditions under the influence of glacier retreat/advance as well as glacial lake formation. Thus, care should be taken when glacier evolution is modeled with a simple parameterization of ice velocity to ice thickness and slope.

Conclusions

We studied changes in ice-flow velocity and surface elevation in Rhonegletscher over the last 100 years. Aerial photographs taken in 1970–2006 were analyzed by photogrammetric techniques to measure the velocity and elevation in the lower half of the glacier. The velocities obtained by this analysis were compared with those measured in 1874–1915 (Mercanton, 1916), which we have digitized in this study. The results showed the changes in glacier dynamics during the rapid retreat from the 19th to the 21st century. The longitudinal strain rate pattern was altered as a result of sub-

stantial changes in the glacier geometry, suggesting that the role of ice dynamics in glacier evolution varies with time. The velocity change from 1970 to 2006 was consistent with the slight thickening in 1970–1981 and subsequent thinning in 1981–2006. However, under the influence of a steepening ice surface from 1981 to 2006, the effect of thinning on the ice velocity was partly canceled out. It is also likely that the changes in the velocity were influenced by subglacial hydraulic conditions. Our data demonstrate that the long-term evolution of the flow velocity is not a simple function of ice thickness and surface slope.

References Cited

Barrand, N. E., Murray, T., James, T. D., Barr, S. L., and Mills, J. P., 2009: Optimizing photogrammetric DEMs for glacier volume change assessment using laser-scanning derived ground-control points. *Journal of Glaciology*, 55(189): 106–116.

Bauder, A., Funk, M., and Huss, M., 2007: Ice-volume changes of selected glaciers in the Swiss Alps since the end of the 19th century. *Annals of Glaciology*, 46: 145–149.

Berthier, E., and Vincent, C., 2012: Relative contribution of surface mass balance and ice flux changes to the accelerated thinning of the Mer de Glace (Alps) over 1979–2008. *Journal of Glaciology*, 58(209): 501–512.

Berthier, E., Schiefer, E., Clarke, G. K. C., Menounos, B., and Remy, F., 2010: Contribution of Alaskan glaciers to sea-level rise derived from satellite imagery. *Nature Geoscience*, 3(2): 92–95, http://dx.doi.org/10.1038/ngeo737.

Canassy, P. D., Bauder, A., Dost, M., Fäh, R., Funk, M., Margreth, S., Müller, B., and Sugiyama, S., 2011: Hazard assessment investigations due to recent changes in Triftgletscher, Bernese Alps, Switzerland. *Natural Hazards Earth System Sciences*, 11: 2149–2162.

Carlen, M. W., 2005: *The Rhone Glacier and its Ice Grotto.* Second edition. Switzerland: Belvedere Furka, 59 pp.

Chen, J., and Funk, M., 1990: Mass balance of Rhonegletscher during 1882/83–1986/87. *Journal of Glaciology*, 36(123): 199–209.

Clarke, G. K. C., 1987: A short history of scientific investigations on glaciers. *Journal of Glaciology*, Special Issue: 4–24.

Cuffey, K. M., and Paterson, W. S. B., 2010: *The Physics of Glaciers.* Fourth edition. Oxford: Elsevier, Butterworth-Heinemann, 693 pp.

Dowdeswell, J. A., and Benham, T. J., 2003: A surge of Perseibreen, Svalbard, examined using aerial photography and ASTER high resolution satellite imagery. *Polar Research*, 22(2): 373–383.

Flotron A., 1924–1998: Jährliche Berichte über die Ergebnisse der Gletschermessungen im Auftrag der Kraftwerke Oberhasli. Unpublished annual reports commissioned by Kraftwerke Oberhasli AG, Flotron AG, Meiringen, Switzerland.

Glaciological Reports, 1881–2011: The Swiss glaciers, 1880–2006/07. ETH Zürich: Laboratory of Hydraulics, Hydrology and Glaciology (VAW), Yearbooks of the Cryospheric Commission of the Swiss Academy of Sciences (SCNAT), volumes 1–128, //glaciology.ethz.ch/swiss-glaciers/.

Goehring, B. M., Vacco, D. A., Alley, R. B., and Schaefer, J. M., 2012: Holocene dynamics of the Rhone Glacier, Switzerland, deduced from ice flow models and cosmogenic nuclides. *Earth and Planetary Science Letters*, 351–352: 27–35.

Herman, F., Anderson, B., and Leprince, S., 2011: Mountain glacier velocity variation during a retreat-advance cycle quantified using sub-pixel analysis of ASTER images. *Journal of Glaciology*, 57(202): 197–207.

Hubbard, B., and Glasser, N., 2005: *Field Techniques in Glaciology and Glacial Geomorphology*: Chichester: John Wiley & Sons, Ltd., 400 pp.

Huss, M., Sugiyama, S., Bauder, A., and Funk, M., 2007: Retreat scenarios of Unteraargletscher, Switzerland, using a combined ice flow mass-balance model. *Arctic, Antarctic, and Alpine Research*, 39(3): 422–431.

Huss, M., Bauder, A., Funk, M., and Hock, R., 2008: Determination of the seasonal mass balance of four alpine glaciers since 1865. *Journal of Geophysical Research*, 113: F01015, http://dx.doi.org/10.1029/2007JF000803.

Iken, A., and Truffer, M., 1997: The relationship between subglacial water pressure and velocity of Findelengletscher, Switzerland, during its advance and retreat. *Journal of Glaciology*, 43(144): 328–338.

Jouvet, G., Huss, M., Blatter, H., Picasso, M., and Rappaz, J., 2009: Numerical simulation of Rhonegletscher from 1874 to 2100. *Journal of Computational Physics*, 228: 6426–6439.

Kääb, A. 2005: Combination of SRTM3 and repeat ASTER data for deriving alpine glacier flow velocities in the Bhutan Himalaya. *Remote Sensing of Environment*, 94(4): 463–474.

Kääb, A., and Funk, M., 1999: Modelling mass balance using photogrammetric and geophysical data: a pilot study at Griesgletscher, Swiss Alps. *Journal of Glaciology*, 45(151): 575–583.

Kääb, A., Haeberli, W., and Gudmundsson, G. H., 1997: Analysing the creep of mountain permafrost using high precision aerial photogrammetry: 25 years of monitoring Gruben Rock Glacier, Swiss Alps. *Permafrost and Periglacial Processes*, 8: 409–426.

Kirkbride, M. P., and Warren, C. R., 1999: Tasman Glacier, New Zealand: twentieth-century thinning and predicted calving retreat. *Global and Planetary Change,* 22(1–4): 11–28.

Krimmel, R. M., 2001: Photogrammetric data set, 1957–2000 and bathymetric measurements for Columbia Glacier, Alaska. U.S. Geological Survey Water-Resources Investigations Report, 01-4089, 46 pp.

Le Meur, E., Gerbaux, M., Schäfer, M., and Vincent, C., 2007: Disappearance of an alpine glacier over the 21st century simulated from modeling its future surface mass balance. *Earth and Planetary Science Letters*, 261: 367–374.

McSaveney, M. J., and Gage, M., 1968: Ice flow measurements on Franz Josef Glacier, New Zealand, in 1966. *New Zealand Journal of Geology and Geophysics*, 11(3): 564–592.

Meier, M. F., Dyurgerov, M. B., Rick, U. K., O'Neel, S., Pfeffer, W. T., Anderson, R. S., Anderson, S. P., and Glazovsky, A. F., 2007: Glacier dominate eustatic sea-level rise in the 21st century. *Science*, 317(5841): 1064–1067.

Mercanton, P. L. (ed.), 1916: Vermessungen am Rhonegletscher/Mensuration au glacier du Rhône: 1874–1915. Zürich: Zücher and Furrer, *Neue Denkschriften der Schweizerischen Naturforschenden Gesellschaft*, 52: 190 pp.

Nuth, C., Mohodt, G., Kohler, J., Hagen, J. O., and Kääb, A., 2010: Svalbard glacier elevation changes and contribution to sea level rise. *Journal of Geophysical Research*, 115: F01008, http://dx.doi.org/10.1029/2008JF001223.

Oerlemans, J., 1986: An attempt to simulate historic front variations of Nigardsbreen, Norway. *Theoretical and Applied Climatology*, 37(3): 126–135.

Paterson, W. S. B., and Savage, J. C., 1963: Geometry and movement of the Athabasca Glacier. *Journal of Geophysical Research*, 68(15): 4513–4520.

Quincey, D. J., Braun, M., Glasser, N. F., Bishop, M. P., Hewitt, K., and Luckman, A., 2011*:* Karakoram glacier surge dynamics. *Geophysical Research Letters,* 38: L18504, http://dx.doi.org/10.1029/2011GL049004.

Scambos, T. A., Dutkiewicz, M. J., Wilson, J. C., and Bindschadler, R. A., 1992: Application of image cross-correlation to the measurement of glacier velocity using satellite image data. *Remote Sensing of Environment*, 42(3): 177–186.

Schneeberger, C., Albrecht, O., Blatter, H., Wild, M., and Hock, R., 2001: Modelling the response of glaciers to a doubling in atmospheric CO_2: a case study of Storglaciaren, northern Sweden. *Climate Dynamics*, 17(11): 825–834.

Span, N., and Kuhn, M., 2003: Simulating annual glacier flow with a linear reservoir model. *Journal of Geophysical Research*, 108(D10): 4313, http://dx.doi.org/10.1029/2002JD002828.

Stroeven, A., van de Wal, R., and Oerlemans, J., 1989: Historic front variations of the Rhône Glacier: simulation with an ice flow model. *In* Oerlemans, J. (ed.), *Glacier Fluctuations and Climatic Change*. Dordrecht: Kluwer Academic Publishers, 391–405.

Sugiyama, S., Bauder, A., Zahno, C., and Funk, M., 2007: Evolution of Rhonegletscher, Switzerland, over the past 125 years and in the future: application of an improved flowline model. *Annals of Glaciology*, 46: 268–274.

Sugiyama, S., Tsutaki, S., Nishimura, D., Blatter, H., Bauder, A., and Funk, M., 2008: Hot water drilling and glaciological observations at the terminal part of Rhonegletscher, Switzerland in 2007. *Bulletin of Glaciological Research*, 26: 41–47.

Tsutaki, S., Nishimura, D., Yoshizawa, T., and Sugiyama, S., 2011: Changes in glacier dynamics under the influence of proglacial lake formation in Rhonegletscher, Switzerland. *Annals of Glaciology*, 52(58): 33–38.

Tsutaki, S., Sugiyama, S., Nishimura, D., and Funk, M., 2013: Acceleration and flotation of a glacier terminus during a proglacial lake formation in Rhonegletscher, Switzerland. *Journal of Glaciology*, 59(215): 559–570.

Turi, G., 2009: *The Short-Term Flow Dynamics of the Rhonegletscher Tongue*. Master thesis, ETH Zürich, Switzerland, 79 pp.

Vincent, C., Soruco, A., Six, D., and Le Meur, E., 2009: Glacier thickening and decay analysis from 50 years of glaciological observations performed on Glacier d'Argentiere, Mont Blanc area, France. *Annals of Glaciology*, 50: 73–79.

Wallinga, J., and van de Wal, R. S. W., 1998: Sensitivity of Rhonegletscher, Switzerland, to climate change: experiments with a one-dimensional flowline model. *Journal of Glaciology*, 44(147): 383–393.

Willis, M. J., Melkonian, A. K., Pritchard, M. E.,and Rivera, A., 2012: Ice loss from the Southern Patagonian Icefield, South America, between 2000 and 2012. *Geophysical Research Letters*, 39: L17501, http://dx.doi.org/10.1029/2012GL053136.

Yamaguchi, S., Naruse, R., and Shiraiwa, T., 2008: Climate reconstruction since the Little Ice Age by modelling Koryto glacier, Kamchatka Peninsula, Russia. *Journal of Glaciology*, 54(184): 125–130.

Zahno, C., 2004: *Der Rhonegletscher in Raum und Zeit: neue geometrische und klimatische Einsichten*. Diplomarbeit, Zürich: ETH Zürich, 131 pp.